FYS4411 - Project 2
The restricted Boltzmannn machine applied to the quantum many body problem

Daniel Heinesen[1], Gunnar Lange[2] & Aram Salihi[2]

[1]Department of Theoretical Astrophysics, University of Oslo, N-0316 Oslo, Norway

[2]Department of Physics, University of Oslo, N-0316 Oslo, Norway

June 7, 2018

Abstract

NICE ABSTRACT! Also check out our GitHub[1]

---

[1]https://github.com/dulte/FYS4411/tree/master/Project2

Contents

1 Introduction

The interest in applying machine learning methods to quantum mechanical system has experienced a veritable surge in recent years, and many different methods and applications are currently being explored (see e.g. [Broecker et al., 2017] or [Botu and Ramprasad, 2015]). A particularly interesting application of machine-learning to the quantum many-body system is presented by [Carleo and Troyer, 2017]. They interpret the quantum many-body wavefunction as a system of exponential complexity, where one is interested in extracting some features, such as the energy. When viewed from this perspective, machine learning algorithms and neural networks are a natural way to attack the problem, as these are methods designed for extracting features from highly complex systems. [Carleo and Troyer, 2017] present a method which they title Neural-network Quantum States (NQS), where they use restricted Boltzmann machines to represent the wavefunction.

We apply their method to a system of fermions in an isotropic harmonic oscillator trap with Coloumb repulsion. This system has the advantage of being well-studied, as both analytic ([Taut, 1994]) and numeric ([Pedersen Lohne et al., 2011]) results are available for selected system configurations. This enables us to benchmark our results, and quantify the goodness of fit of the NQS to the quantum many-body problem.

We focus on the ground state of our system, and therefore only investigate the case of 1 and 2 electrons, in 1, 2 and 3 dimensions. We use restricted Boltzmann machines to attain the form of our wavefunction, and the use Variational Monte Carlo (VMC) methods to establish an upper bound on the ground state energy. The weights and biases in our neural network are minimized using a stochastic gradient approach with a fixed learning rate. We compare three different sampling methods in our VMC calculations - Metropolis sampling, importance sampling and Gibbs sampling. For each of these methods, we investigate how our system behaves as we vary the parameters associated with the system, and try to find an optimal parameter configuration for the 1D case with one particle and for the 2D case with two particles. We also include an estimation of the statistical errors involved, using the blocking method.

2 Theory

2.1 The Hamiltonian

We consider a D-dimensional system of P electrons confined in an isotropic harmonic oscillator trap. Working in natural units ($\hbar = c = e = m_e = 1$), the Hamiltonian of such a system is given by:

$$H = \sum_{i=1}^{P}\left(-\frac{1}{2}\nabla_i^2 + \frac{1}{2}\omega^2 r_i^2\right) + \sum_{i=1}^{P}\sum_{j=1}^{i}\frac{1}{r_{ij}} \tag{1}$$

Here ω is the frequency of the oscillator trap, r_i is the D-dimensional position vector of electron i and $1/r_{ij}$ is the distance between electron i and j. We fix $\omega = 1$ throughout this investigation. The first term of the Hamiltonian describes the interaction of the electrons with the potential, and we refer to it as the noninteracting part. The second term describes the Coloumb interaction between the electrons, and we refer to it as the interacting part.

We now wish to find the energy, E of our system, by solving the time-independent Schrödinger equation:

$$H\Psi = E\Psi \tag{2}$$

Where Ψ is the wavefunction of the system.

2.2 Analytic solution

We are chiefly interested in the ground-state energy of our system, as this is the state that the system will fall into if left unperturbed by e.g. thermal excitation. If we ignore the interacting part, then we have an analytic solution to the ground-state wavefunction for two electrons, which according to [Griffiths, 2004] is given by:

$$\psi(r_1, ..., r_P) = C \exp\left(-\frac{\omega}{2} \sum_{i=1}^{P} r_i^2\right) \tag{3}$$

Where C is a normalization constant. Furthermore, the ground-state energy (in natural units) of such a system is given by:

$$\frac{E}{\omega} = P\frac{D}{2} \tag{4}$$

Note, however, that all of the above expressions are only valid up to $P = 2$, as we are dealing with spin-1/2 fermions, to which the Pauli exclusion principle applies. Therefore, we can only have two particles in the ground-state, and these particles must have opposite spin. More precisely, they must be in the singlet state (total spin 0) in the noninteracting case, as discussed in appendix B. In what follows, we therefore restrict ourselves to $P \in \{1, 2\}$.

We also have analytic results for some special cases in the interacting case. In particular, according to [Taut, 1994] and [Pedersen Lohne et al., 2011], the energy is 3 (in natural units) for 2 particles in the 2-dimensional case with $\omega = 1$.

2.3 The variational principle

In the general case, where analytic solutions are not available, it is desirable to use a numeric method to find the ground state energy, or at least an upper bound on the ground state energy. We achieve such an upper bound by invoking the variational principle, as formulated in [Griffiths, 2004], which states that:

$$E_0 \leq \frac{\langle\Psi_T|H|\Psi_T\rangle}{\langle\Psi_T|\Psi_T\rangle} \tag{5}$$

Where E_0 is the ground-state energy and Ψ_T is any (not necessarily normalized) trial wavefunction for our system. We therefore choose a class of trial wavefunctions, Ψ_T, and then compute $E' = \langle\Psi_T|H|\Psi_T\rangle/\langle\Psi_T|\Psi_T\rangle$ by using a Monte Carlo approach. The variational method then guarantees that our approximation to the energy, E' will be larger than the ground state energy E_0. We then adjust our trial wavefunction within our class of wavefunctions, to give the lowest possible energy, hoping to attain a decent estimate for the actual ground-state energy of our system.

2.4 Neural-network quantum states and Restricted Boltzmann Machines

To actually determine our class of trial wavefunction, we follow the approach outlined by [Carleo and Troyer, 2017]. They choose to interpret the problem of solving equation 2 as a multi-dimensional minimization and feature extraction problem. As neural networks were designed to tackle exactly this class of problem, we choose to employ a neural network to find our trial wavefunction.

We choose, as done by [Carleo and Troyer, 2017] a restricted Boltzmann machine (RBM) as the basis for our neural network. Restricted Boltzmann Machines (RBM) are described in great detail in the literature, see e.g. [Hinton, 2010]. We therefore provide only a rough outline on how to apply them. We begin by setting up a vector of M visible nodes, $\mathbf{X}$, which corresponds to the position states of our system (with one state per particle, P and dimension, D, i.e. $M = PD$), and a vector of N hidden nodes, $\mathbf{H}$ which correspond to some feature of our system that we

wish to use to predict our wavefunction. Each of these nodes have a bias associated with them, which determine their relative importance. Additionally, there are also weights associated with connections between the hidden nodes and the visible nodes, but there are no connections between nodes in the same layer (hence *restricted* Boltzmann machine). The RBM method then consists of modelling the probability distribution for our system, given some visible nodes $\mathbf{X}$ and some hidden nodes $\mathbf{H}$, by a Boltzmann distribution function of the form:

$$F_{rbm}(\mathbf{X}, \mathbf{H}) = \frac{1}{Z} \exp\left(-\frac{1}{T_0} E(\mathbf{X}, \mathbf{H})\right) \tag{6}$$

Where Z is a normalization constant and T_0 is some reference temperature (set to 1 in what follows). The energy, $E(\boldsymbol{X}, \boldsymbol{H})$ relates the weights and biases to the probability distribution. In the standard RBM formulation, both $\boldsymbol{X}$ and $\boldsymbol{H}$ are binary variables. We choose the hidden nodes $\boldsymbol{H}$ to be binary, $h_i \in \{0, 1\}$. The visible nodes, $\boldsymbol{X}$, however, represent the position of the electrons in our system, and must therefore be modelled as a continuous function. We therefore use an extension of standard RBM known as Gaussian-Bernoulli Deep Boltzmann Machine's (GDBM), as described by [Wang et al., 2014] (and also used by [Carleo and Troyer, 2017]). They implement the energy as:

$$E(\mathbf{X}, \mathbf{H}) = \sum_{i=1}^{M} \frac{(X_i - a_i)^2}{2\sigma^2} - \sum_{j=1}^{N} b_j H_j - \sum_{i=1}^{N} \sum_{j=1}^{M} \frac{X_i w_{ij} H_j}{\sigma^2} \tag{7}$$

Where a_i is the bias associated with the visible node X_i, b_i is the bias associated with the hidden node H_i and w_{ij} is the weight associated with the coupling between X_i and H_j. As discussed in [Wang et al., 2014], this makes the marginal distribution of the h_i a Bernoulli distribution, whereas the marginal distribution of X_i form a normal distribution with variance σ^2. In what follows, we fix $\sigma = 1$.

As our wavefunction is a function of the position coordinates only, we choose to interpret the marginal distribution of the visible nodes as our wavefunction. This marginal distribution is given by:

$$F_{rbm}(\mathbf{X}) = \sum_{h_i \in \mathbf{H}} F_{rbm}(\mathbf{X}, \mathbf{H}) \tag{8}$$

Which gives, after some algebra done in [Hjorth-Jensen, 2018], our class of trial wavefunctions as:

$$\Psi_T(\mathbf{X}) = F_{rbm}(\mathbf{X}) = \frac{1}{Z} \exp\left(-\sum_{i=1}^{M} \frac{(X_i - a_i)^2}{2\sigma^2}\right) \prod_{j=1}^{N} \left(1 + \exp\left(b_j + \sum_{i=1}^{M} \frac{X_i w_{ij}}{\sigma^2}\right)\right) \tag{9}$$

This trial wavefunction, given biases and weights a, b, w, is then plugged into equation 5 to find an upper bound on the ground-state energy of our system. We seek to optimize this wavefunction with respect to a, b and w.

2.5 Variational Monte Carlo methods

Having established our trial wavefunction, it remains to use the variational principle to estimate the ground state energy. We use a Monte Carlo approach to estimate the inner product given in equation 5. A more detailed description of this may be found in [Hjorth-Jensen, 2015], and we therefore only sketch a procedure. We begin by considering the probability distribution associated with our trial wavefunction, given by:

$$P(\mathbf{X}) = \frac{|\Psi_T|^2}{\int d\mathbf{X} |\Psi_T|^2} \tag{10}$$

Where the normalization integral is to be carried out over all particles and dimension (i.e. over M variables). If we now define the local energy (by solving equation 2 for E) as:

$$E_L(\mathbf{X}) = \frac{1}{\Psi_T} H \Psi_T \tag{11}$$

Then the expectation value of the Hamiltonian (which gives the energy) is given by:

$$E_0 \leq E[H] = \int d\mathbf{X} P(\mathbf{X}) E_L(\mathbf{X}) \approx \frac{1}{K} \sum_{i=1}^{K} E_{L,i} \tag{12}$$

Thus, we can get an approximation to the ground state energy by averaging the local energy for various system configurations. This method is, however, contingent upon our ability to efficiently compute the local energy and sample the position space.

2.6   The local energy

The local energy is defined in equation 11, with the Hamiltonian given in equation 1. Note that the most complicated part of this expression is the second derivative of the wavefunction. We derive an analytic expression for this is in appendix A.1. There, we show that the local energy is given by:

$$\frac{1}{\Psi_T} H\Psi_T = -\frac{1}{2} \sum_{k=1}^{M} \left[\frac{a_k - X_k}{\sigma^2} + \sum_{j=1}^{N} \frac{w_{kj}}{\sigma^2 \left(1 + \exp\left(-b_j - \sum_{i=1}^{M} \frac{X_i w_{ij}}{\sigma^2}\right)\right)} \right]^2$$
$$+ \frac{M}{2\sigma^2} - \frac{1}{2} \sum_{k=1}^{M} \sum_{j=1}^{N} \frac{w_{kj}^2 \exp\left(-b_j - \sum_{i=1}^{M} \frac{X_i w_{ij}}{\sigma^2}\right)}{\sigma^4 \left(1 + \exp\left(-b_j - \sum_{i=1}^{M} \frac{X_i w_{ij}}{\sigma^2}\right)\right)^2} + \frac{1}{2} \sum_{i=1}^{M} \omega^2 X_i^2 + \sum_{i=1}^{P} \sum_{j=1}^{i} \frac{1}{r_{ij}} \tag{13}$$

2.7   Sampling the position space

To make sense of equation 12, we must sample our position space, to get a good estimate for the local energy of the system. We employ three different sampling techniques.

2.7.1   The Metropolis algorithm

The Metropolis algorithm is described in further detail in [Hjorth-Jensen, 2015]. We begin by noting that the wavefunction gives the probability of finding the particle at a point in position space. We will therefore get the most reliable estimates for our local energy if we sample where the wavefunction (and thus the probability distribution) is large, and we then avoid wasting CPU cycles. The Metropolis algorithm is one way to achieve this. This involves proposing to move a single particle according to:

$$\boldsymbol{r}_{\text{i,new}} = \boldsymbol{r}_{\text{i}} + \boldsymbol{\xi} dx \tag{14}$$

Where $\boldsymbol{r}_{\text{i}}$ is the position of particle i, dx is step size which we tune and $\boldsymbol{\xi}$ is a D-dimensional vector of random numbers, whose distribution we discuss in section 3.3. To find out whether we should sample local energy at this new position, we compute the ratio:

$$\Theta = \frac{P(\boldsymbol{X}_{\text{new}})}{P(\boldsymbol{X})} = \frac{|\Psi(\boldsymbol{X}_{\text{new}})|^2}{|\Psi(\boldsymbol{X})|^2} \tag{15}$$

Where $\boldsymbol{X}_{\text{new}}$ is the position of the particles after updating the position of particle i according to 14. Note that this ratio determines if the particle is more likely to be found at the position $\boldsymbol{X}_{\text{new}}$ than at position $\boldsymbol{X}$. The move is only accepted if $\Theta \geq \theta$, where $\theta \in [0, 1]$ is a uniformly distributed random variable. Thus, if the probability of finding the particle at $\mathbf{X}_{\text{new}}$ is larger than the probability of finding the particle at $\mathbf{X}$, then we accept the move. If not, then the larger the energy difference the less probable it is that the move is accepted. As such, we should eventually end up moving fairly close to the most likely position, without getting stuck in it.

2.7.2 The Metropolis-Hasting alogrithm/importance sampling

We compare the Metropolis algorithm to an alternative, known as importance sampling or Metropolis-Hasting. This is described in further detail in [Hjorth-Jensen, 2015]. Note that the Metropolis sampling described in the previous section picks positions at random, and as such does not have a preference for proposing steps that move the system to a region of high probability density (given by $|\Psi|^2$). As such, some CPU cycles will be wasted on positions that have a very small probability of occurring, and will never be accepted. Importance sampling seeks to alleviate this problem by introducing a quantum force, which "pushes" the system in the direction of high probability. This changes the way a new step is proposed, as discussed in section 3.3. This force is, on particle i given by:

$$F_i(\boldsymbol{X}) = \frac{2}{\Psi_T} \nabla_i \Psi_T = 2\nabla_i \log \Psi_T \tag{16}$$

We compute this in appendix A.1 and show there that this force is given by:

$$F_i(\boldsymbol{X}) = 2\sum_{k=1}^{D}\left(\frac{a_k - X_k}{\sigma^2} + \sum_{j=1}^{N}\frac{w_{kj}}{\sigma^2\left(1 + \exp\left(-b_j - \sum_{i=1}^{M}\frac{X_i w_{ij}}{\sigma^2}\right)\right)}\right) \tag{17}$$

The analysis in [Hjorth-Jensen, 2015] shows that the correct way to include this in our algorithm (in addition to modifying our proposed step as discussed in section 3.3) is by multiplying the transition probability w defined in equation 15 by a Green's function given by:

$$G(\mathbf{X}, \mathbf{X}') = \frac{1}{(4\mathcal{D}dx')^{3/2}}\sum_{i=1}^{M}\exp\left(-\frac{(X_i - X_i' - \mathcal{D}dx'F_i(\mathbf{X}'))^2}{4\mathcal{D}dx'}\right) \tag{18}$$

Where $\mathcal{D}$ is a diffusion parameter, which in our case equals $1/2$, and dx' is a step size which may be different from the step size for brute-force sampling, and which we tune. The modified transition probability is given by:

$$w_{\text{importance}} = \frac{|\Psi(\boldsymbol{X}_{\text{new}})|^2}{|\Psi(\boldsymbol{X})|^2}\frac{G(\boldsymbol{X}, \boldsymbol{X}_{\text{new}})}{G(\boldsymbol{X}_{new}, \boldsymbol{X})} \tag{19}$$

This transition probability is implemented exactly as in the previous section.

2.7.3 Gibbs Sampling

Gibbs sampling is an alternative to Metropolis/Metropolis-Hastings algorithm, which is described in greater detail in [Wang et al., 2014]. Here we have a more direct connection between the probability distribution of the neural network and the wavefunction. In order to establish a direct physical connection to the probability distribution of the RBM, we now model our wavefunction as:

$$\Psi_{T,\text{Gibbs}} = \sqrt{F_{rbm}(\boldsymbol{X})} \tag{20}$$

Where Ψ_T is given in equation 9. Note that, as the wavefunction is real-valued, this implies $|\Psi_{T,\text{Gibbs}}(\boldsymbol{X})|^2 = F_{rbm}(\boldsymbol{X})$, i.e. the marginal distribution directly models the position probability distribution.

We are also interested in the conditional distribution of the hidden nodes. This gives, after a few lines of Algebra done in [Hjorth-Jensen, 2018]:

$$\begin{aligned}P(H_j = 1|\boldsymbol{X}) &= \frac{1}{1 + \exp\left(-b_j - \frac{1}{\sigma^2}\sum_{i=1}^{M}X_i w_{ij}\right)}\\[2mm]P(H_j = 0|\boldsymbol{X}) &= \frac{1}{1 + \exp\left(b_j + \frac{1}{\sigma^2}\sum_{i=1}^{M}X_i w_{ij}\right)}\end{aligned} \tag{21}$$

We now initialize the weights, biases and position $\boldsymbol{X}$, as discussed in section 3.2. We can then compute the marginal distributions for $\boldsymbol{X}$ given in equation 21. We then draw a uniform random number $\theta \in [0, 1]$ for each H_i, and update H_i according to equation 21. Then the positions are updated according to their conditional distribution, which is, as shown in [Hjorth-Jensen, 2018] is:

$$X_i \sim \mathcal{N} \left(\sum_{j=1}^{N} w_{ij} H_j, \sigma^2 \right) \tag{22}$$

We then compute the local energy using this $\boldsymbol{X}$. Note that we here cannot use equation 11, as this is only valid for $\Psi_T = F_{rbm}(\boldsymbol{X})$. However, the new expression for local energy only differs by some numerical factors to the previous expression, as discussed in detail in appendix A.3.

2.8   Optimizing our wavefunction in parameter space

For our neural network to be successful, we must be able to minimize the energy of our wavefunction. This is done by varying the parameters a_i, b_i and w_{ij}, and computing the local energy. The variational method then guarantees that the lowest energy we find will be larger than the ground state energy. We employ a stochastic gradient method to find the minimum in our parameter space. Defining a vector of all parameters, $\boldsymbol{\theta}$, we iterate this vector according to:

$$\boldsymbol{\theta}^{i+1} = \boldsymbol{\theta}^i + \gamma \frac{\partial \overline{E}_L}{\partial \boldsymbol{\theta}^i}(\boldsymbol{\theta}^i) \tag{23}$$

Where $\overline{E}_L$ is the energy computed by means of the variational Monte Carlo method (given by equation 12) and γ is the step size, which we vary. The derivative is with respect to all parameters. It is shown in [Heinesen et al., 2018] that the derivative of this expectation value of the energy is given by:

$$\frac{\partial \overline{E}_L}{\partial \boldsymbol{\theta}}(\boldsymbol{\theta}) = 2 \left(\left\langle \frac{1}{\Psi_T} \frac{\partial \Psi_T}{\partial \boldsymbol{\theta}} \overline{E}_L(\boldsymbol{\theta}) \right\rangle - \left\langle \frac{1}{\Psi_T} \frac{\partial \Psi_T}{\partial \boldsymbol{\theta}} \right\rangle \left\langle \overline{E}_L(\boldsymbol{\theta}) \right\rangle \right) \tag{24}$$

We must therefore compute the derivative of our trial wavefunction, given in equation 9, with respect to all of our variational parameters. This is done in detail in appendix A.2 for Metropolis/importance sampling and in appendix A.3 for Gibbs sampling. We iterate this method until the absolute value of our gradient, $\frac{\partial \overline{E}_L}{\partial \boldsymbol{\theta}}$ is smaller than a threshold ϵ, or we have reached some maximum iteration count.

3   Methods

3.1   An overview of the structure of our program

Our entire program may be found on our GitHub[2]. It is an extension of the program presented in [Heinesen et al., 2018]. The program consists of 3 main classes:

`main.cpp`   The main class first reads in the parameter files. It then sets up the initial guess for the weights of the neural networks and runs the stochastic descent method. Finally, it runs the full simulation with the optimized weights.

`simulation.cpp`   This class contains the minimization method itself, and also runs the main Monte Carlo loop.

---

[2]`https://github.com/dulte/FYS4411/tree/master/Project2`

`system.cpp` The system class contains all the functions for the wavefunction, the different sampling methods, and the acceptance checks. It also contains the function for computing the local energy and the derivatives of the wavefunction as a function of the various parameters.

In addition, we implement various auxiliary classes, that read in parameters, dump variables to file and do statistical analysis. These are described in greater detail on our repository.

3.2 Initializing our system

3.2.1 Initializing the position

To initialize our system, we must distribute our particles. How we distribute the particles, however, depends on the sampling method employed. When using the Metropolis algorithm or Gibbs sampling, we distribute our particles according to:

$$\boldsymbol{r}_i = \boldsymbol{\xi} \tag{25}$$

Where $\boldsymbol{\xi}$ is a vector of D number, normally distributed with $\xi \sim 0.5\mathcal{N}(0,1)$ as we find that this gives a good spread.

When using importance sampling, however, we must distribute our particles slightly differently, as discussed in [Hjorth-Jensen, 2015]. In this case, the initial distribution of particles is given by:

$$\boldsymbol{r}_i = \boldsymbol{\xi}'\sqrt{dx'} \tag{26}$$

Where $\boldsymbol{\xi}'$ is a vector of D number distributed as $\mathcal{N}(0,1)$ and dx' is the step size discussed earlier, which we tune, as described further in section 3.6.

3.2.2 Initializing the parameters

We wish to minimize our wavefunction as a function of the biases a, b and the weights w. This is done by iterating equation 23. However, we require an initial guess for the vector of parameters, $\boldsymbol{\theta}^0$. We choose this initial guess to be distributed as $\mathcal{N}(0, 0.5)$.

3.2.3 Initializing the simulation

To initialize the simulation, we set the parameters in the parameter file found on our GitHub[1]. This gives the option to set a number of parameters of the system. Specifically, the parameter file allows the following parameters to be set at runtime:

- The number of Monte Carlo cycles

- The number of particles, P

- The number of hidden nodes, N

- The number of dimensions, D

- The oscillator frequency ω

- The spread in the visible nodes σ

- The diffusion parameter D (setting this to 0 deactivates importance sampling)

- The step size, dx

- The learning rate, γ

- Whether or not the system is interacting

- Whether the energy should be computed numerically or analytically

- Whether or not to use Gibbs sampling

3.3 Proposing a new position

As discussed in section 2, both the Metropolis algorithm and the Metropolis-Hasting algorithm rely on proposing a new position of the system. The general form for this updating was given in equation 14. We now discuss how this is concretely implemented for the different sampling method.

For straightforward Metropolis sampling, there is no bias in selecting this position. We therefore simply define the new position by:

$$\boldsymbol{r}_{\text{i,new}} = \boldsymbol{r}_i + \boldsymbol{\xi} dx \tag{27}$$

Where $\boldsymbol{\xi}$ consists of D numbers, uniformly distributed in $[-1, 1]$ and dx is a step size.

For importance sampling, we add a bias in selecting the new position. This bias is introduced by including the quantum force, presented in equation 17. The details of how to implement this bias are presented in [Hjorth-Jensen, 2015]. This gives that the new step should be selected according to:

$$\boldsymbol{r}_{\text{i,new}} = \boldsymbol{r}_i + \boldsymbol{\xi}'\sqrt{dx'} + \mathcal{D}\boldsymbol{F}_i dx \tag{28}$$

Where $\boldsymbol{F}_i$ is the quantum force on particle i, $\mathcal{D}$ is the diffusion parameter (equal to $1/2$) and $\boldsymbol{\xi}' \sim \mathcal{N}(0, 1)$, and dx' is the step size for importance sampling discussed earlier.

3.4 Implementing the optimization of the biases and the weights

To find the best trial wavefunction, we run the optimization algorithm given in equation 23 until the absolute value of the gradient is less than some ϵ, or we have surpassed 100 iterations. We use 10 times fewer Monte Carlo cycles to compute the local energy in the optimization loop than in the actual simulation used to determine the energy, and set ϵ according to what convergence we observe.

3.5 The errors in our energy

We wish to provide error bounds on the energies that we find. Note that the local energies constitute a highly correlated system (a time series), as the state of the system in the current Monte Carlo step differs only by the position of a single particle from the state in the previous Monte Carlo step. The variance of the energy is therefore not a good indicator of the error in our system. Instead, we use a technique known as blocking. This is described in further detail in [Jonsson, 2018] and we follow the same procedure as outline in [Heinesen et al., 2018].

Blocking works by averaging successive observations of the local energy. Such a pairwise operation preserves the variance of the data, but reduces the covariance of the data. We keep doing this until the covariance is small enough, as described in detail in [Jonsson, 2018]. To ensure that we can this as frequently as possible, we let our number of Monte Carlo cycles be a power of 2.

3.6 Tuning the parameters

We note that our results are contingent upon a number of parameters, in addition to the biases and weights that our minimization algorithm tunes, and our choice for initial distribution of the particles and the parameters. Specifically, we must choose the learning rate, γ, the step size dx, the number of hidden nodes N and the number of Monte Carlo cycles.

We tune each of these parameters in turn, hoping to get close to a global optimum in parameter space without having to do a complete stochastic descent. Note that the step size γ and the number of hidden nodes N are intimately related, as γ determines the rate of convergence whereas N determines the dimensionality of the convergence problem. We therefore choose to tune these parameters simultaneously, as they strongly influence one another.

3.6.1 Tuning the step size, dx

The step size dx determines how well we are able to sample the position space, as it describes how far our proposed next position should be from the previous position. To find the best possible step size dx, we investigate the behavior of the energy for different dx, and look at the acceptance rate. For this analysis, we fix some values of γ and N that give acceptable values. We then choose a dx that gives a good estimate of the energy, whilst having neither an extremely high nor an extremely high acceptance rate, as a low acceptance rate implies that we waste a large amount of CPU cycles, whilst a high acceptance rate implies that the system may get stuck.

We first do this for the simplest possibles system (1 particle in 1 dimension), checking both the brute-force Metropolis sampling and importance sampling (note that Gibbs sampling does not use a dx).

We also do the same analysis for 2 particles in 2 dimensions, including interaction, as we have analytic answers for this system available in [Taut, 1994].

3.6.2 Tuning the learning rate, γ and the number of hidden nodes, N

We choose to tune the learning rate γ and number of hidden nodes N simultaneously, as explained above. We choose the values for dx found previously, and look at the absolute value of the gradient and the energy as a function of number of minimization iterations. We then choose the combination of parameters that gives a good combination of low gradient and low energy. We do this separately for Metropolis sampling, importance sampling and Gibbs sampling, and separately for the simplest system (1 particle 1 dimension) and the interacting system (2 particles, 2 dimensions with interaction).

3.6.3 Choosing the number of Monte Carlo steps

Note that the numbers of Monte Carlo steps required will depend on the method used to sample the space, as e.g. importance sampling will accept more steps and therefore require fewer cycles. As we are limited to 2 particles, however, we can afford to use a fairly large number of Monte Carlo cycles. We therefore choose to use enough Monte Carlo steps to ensure convergence in the uncertainty in the energy, and use the same number of Monte Carlo cycles independent of the sampling method. We find by trial and error that 2^{21} are sufficiently Monte Carlo steps to ensure convergence.

3.7 Benchmarking our results

Having chosen the parameters of our system, we can now benchmark our results. We attempt to look at the ground state energy for 1 and 2 particles, in 1,2 and 3 dimensions, both with and without interaction. Note that we have analytic results for the noninteracting case, given by equation 4, and that we have analytic results in the interacting case with 2 dimension.

Note, that the variational principle only guarantees that we attain an upper bound on the ground state energy. As such, we can only check that our result is larger than or equal to the analytic result, and how close we are to the exact result.
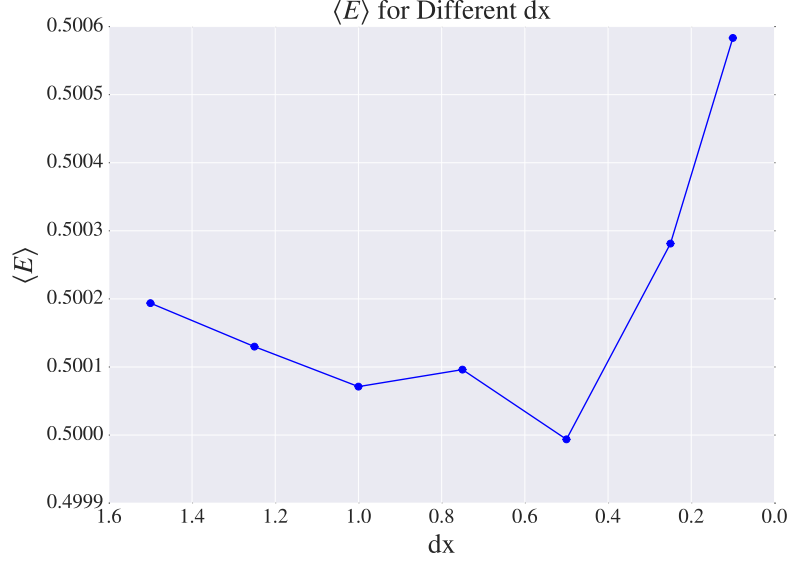
4 Results

4.1 Tuning our neural network quantum state in the simplest system
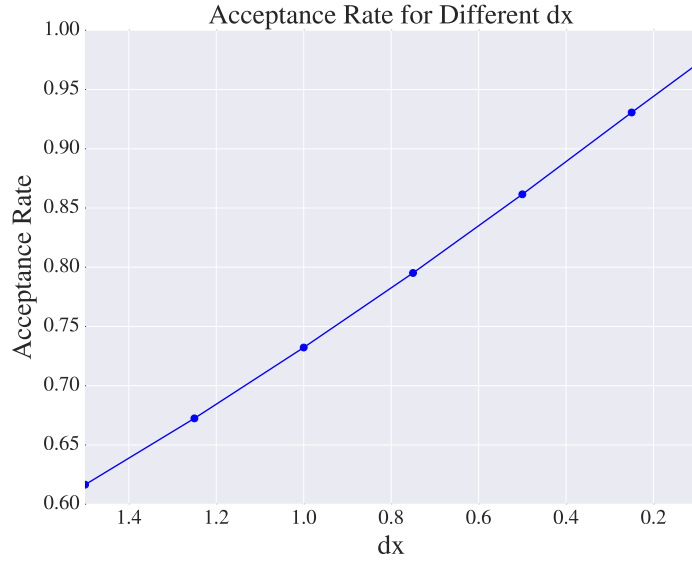
We begin by tuning the parameters of our NQS in the simplest possible case (1 dimension with 1 particle).

4.1.1   Tuning dx

We show the energy and acceptance rate using brute-force Metropolis sampling for various step sizes in figure 1 below:
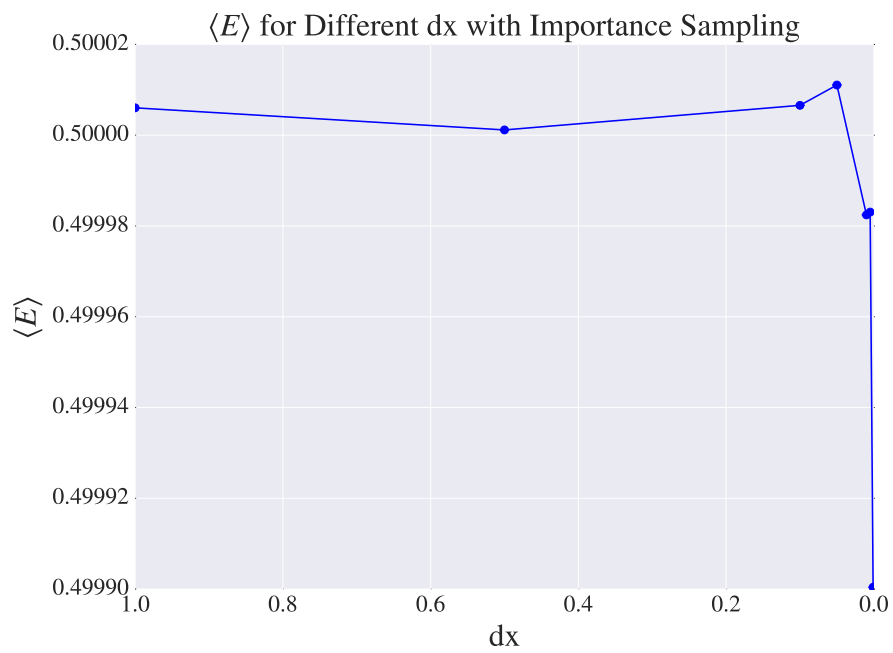

(a) Mean energy

(b) Acceptance rate

Figure 1: Plot of the mean energy and corresponding acceptance rate for various values of dx, using 1 particle in 1 dimension and $2^{21}/10$ Monte Carlo steps. This was produced using brute-force Metropolis sampling with $N = 2$ and $\gamma = 0.3$. Errors were estimated using blocking, but are too small to be visible.

As explained in section 5.1.1, we choose $dx = 0.5$. The equivalent plot with importance sampling is shown in figure 2. In the case of importance sampling, we choose $dx = 0.5$ (see 5.1.1).
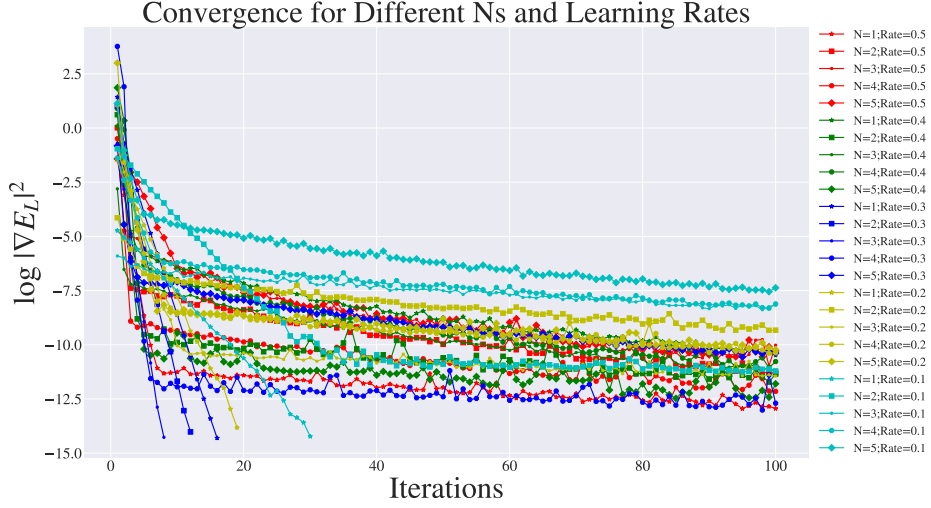
(a) Mean energy
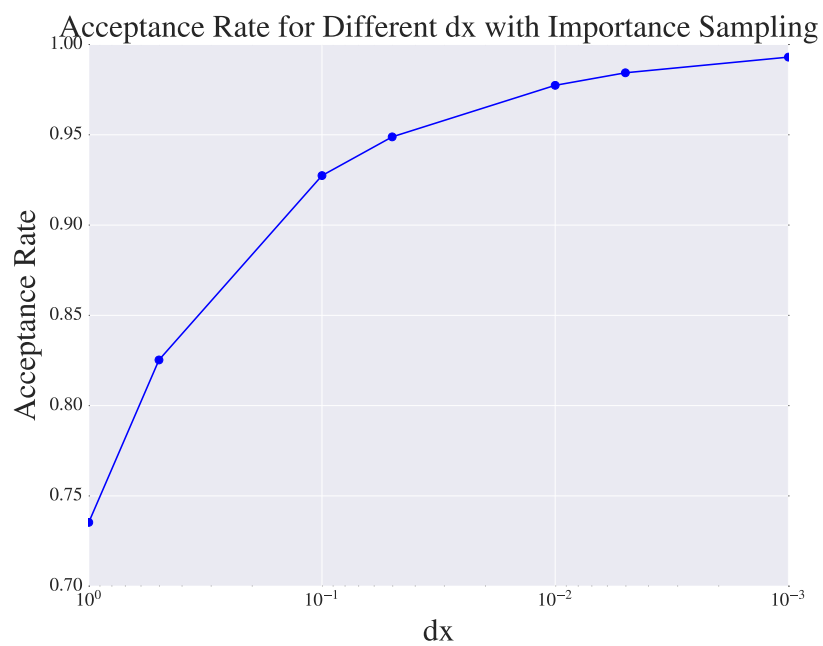
(b) Acceptance rate

Figure 2: Same as figure 1, but using importance sampling

4.1.2 Tuning N and γ

As discussed in section 3.6.2, we tune the learning rate, γ and the number of hidden nodes, N together. This gives the plot shown in figure 3 for the brute-force Metropolis algorithm. As explained in section 5.1.1, we here choose $\gamma = 0.3$ and $N = 2$.

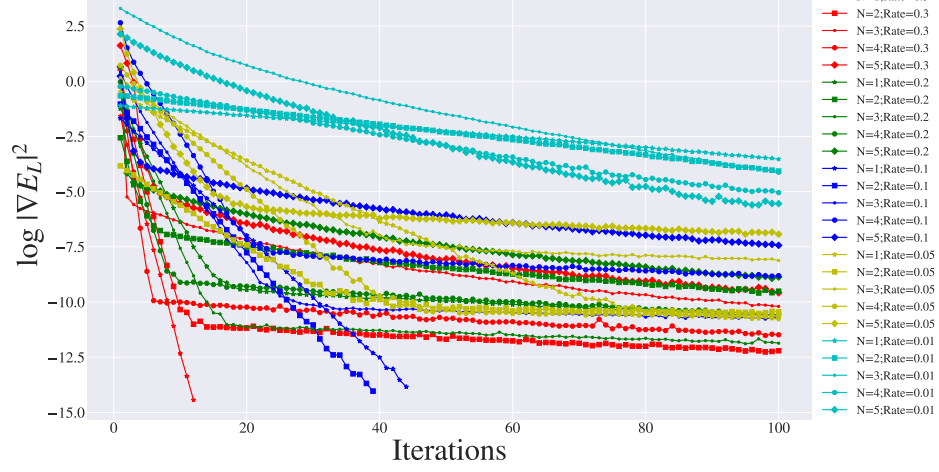(a) The natural logarithm of the square gradient of the local energy.
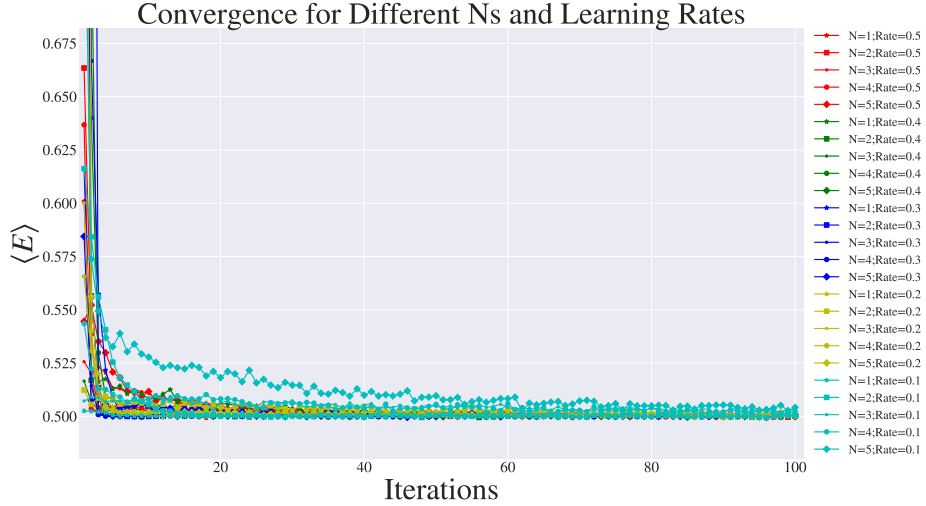
(b) Energy

Figure 3: Plot of the absolute value of the gradient and the energy as a function of iterations for various values of N and γ. This was performed using brute-force Metropolis sampling, with 1 particle in 1 dimension and $2^{21}/10$ Monte Carlo cycles. We used $dx = 0.5$. Our convergence tolerance ϵ was 10^{-5}, and we used a maximum of 100 iterations.
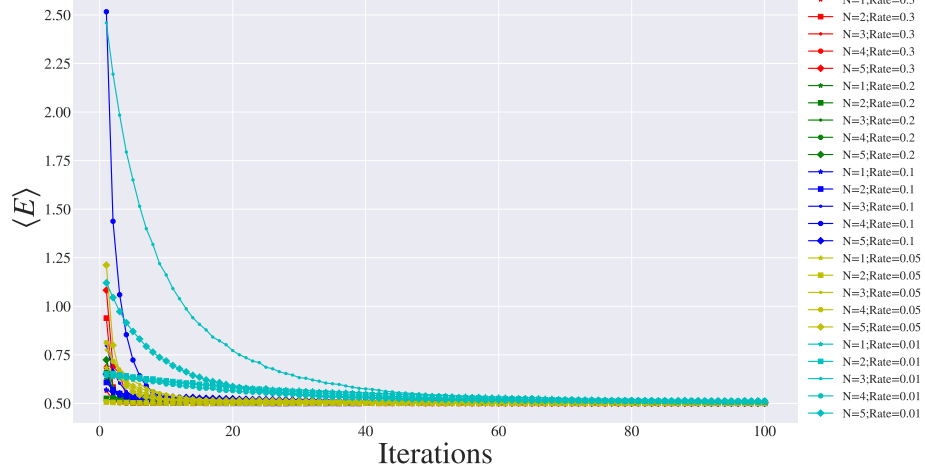
The equivalent plot for importance sampling is shown in figure 4. As explained in section 5.1.1, we here choose $N = 2$ and $\gamma = 0.3$.

(a) The natural logarithm of the square gradient of the local energy.
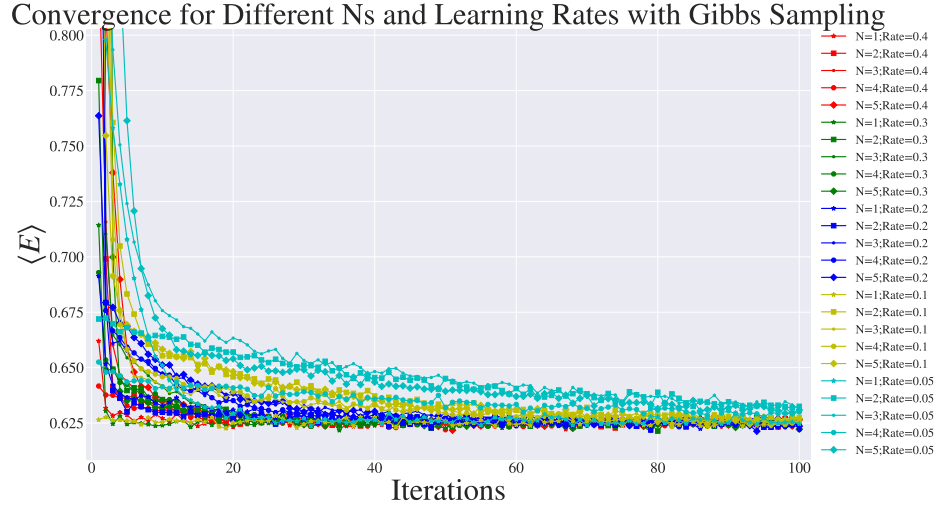

(b) Energy

Figure 4: Same as figure 3, but using importance sampling.

Finally, the same plot for Gibbs sampling is shown in figure 5. As explained in section 5.1.1 we here choose $N = 2$ and $\gamma = 0.35$.
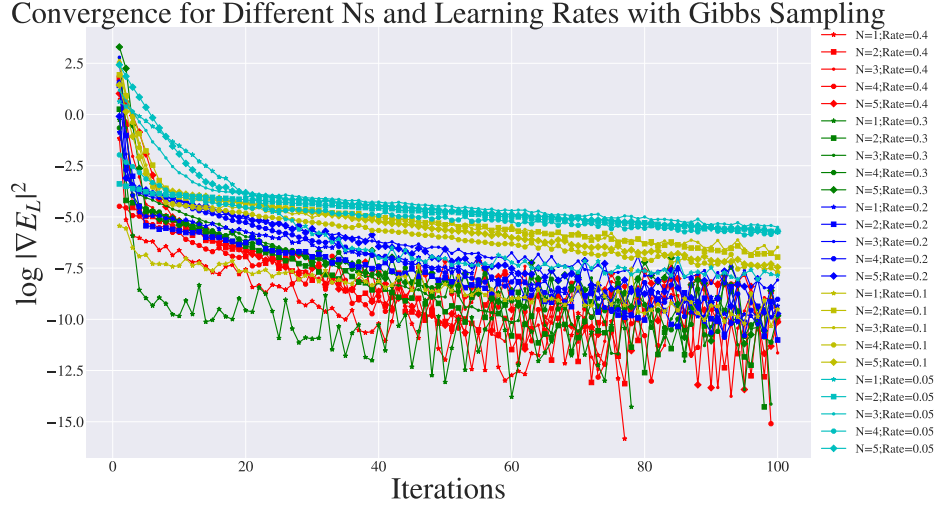
(a) The natural logarithm of the square gradient of the local energy.

(b) Energy

Figure 5: Same as figure 3 but using Gibbs sampling

4.2 Tuning our neural network quantum state in the interacting system

We perform the same analysis as in the previous section also in the interacting system with 2 particles in 2 dimension.

4.2.1 Tuning dx

We show the results of tuning the step size in the interacting case in figure 6. As explained in section 5.1.2 we choose $dx = 1$ in this case.
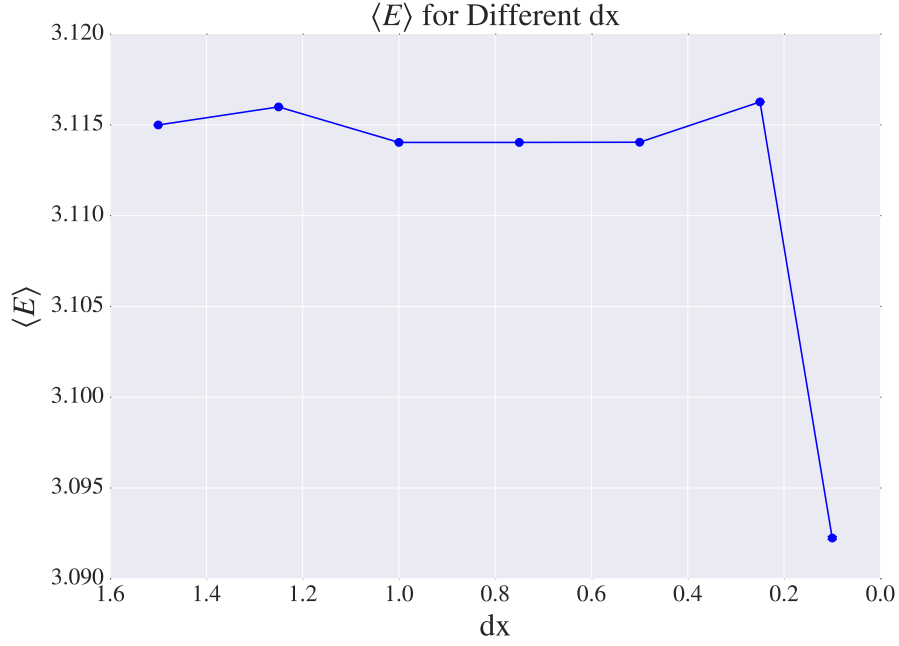
(a) Mean of the energy
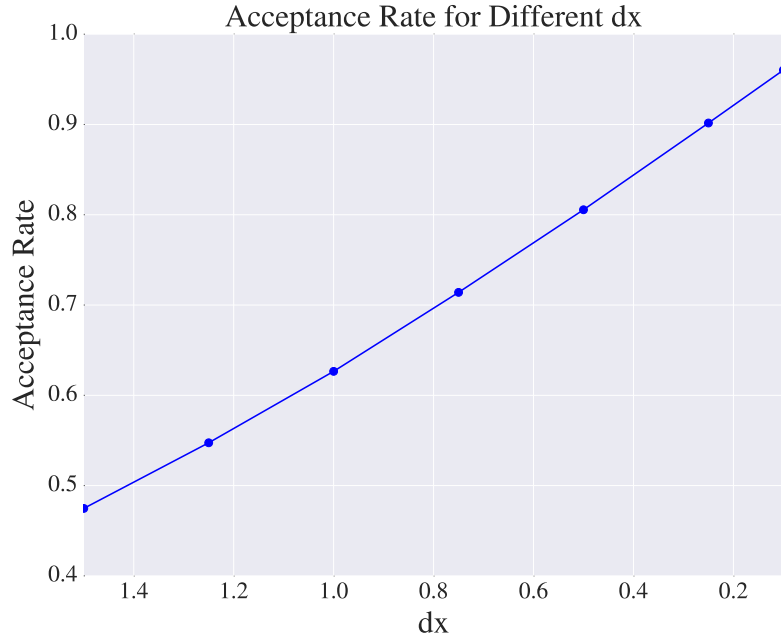
(b) Acceptance ratio

Figure 6: Plot of the mean energy and corresponding acceptance rate for various values of dx using 2 particles in 2 dimensions and $2^{21}/10$ Monte Carlo steps. This was produced using brute-force Metropolis sampling with $N = 2$ and $\gamma = 0.3$.

We show the equivalent plot with importance sampling in figure 7. As explained in section 5.1.2,

we choose $dx = 0.1$ in this case.
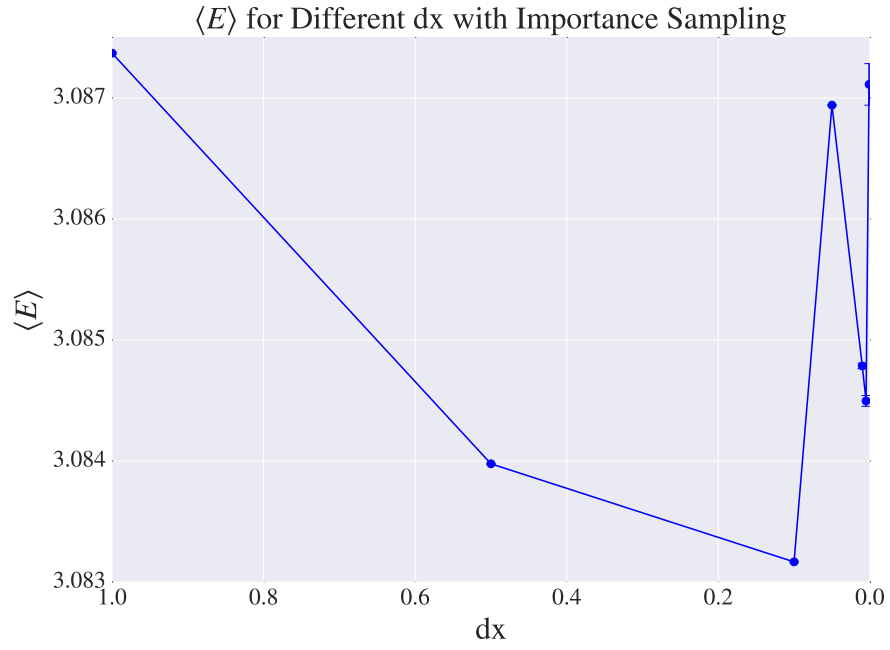
(a) Mean of the energy

(b) Acceptance ratio

Figure 7: Same as figure 6 but with importance sampling

4.2.2 Tuning N and γ

Tuning of the learning rate γ and N gives the plot shown in figure 8 for the brute-force Metropolis algorithm. As explained in section 5.1.2, we here choose $N = 2$ and $\gamma = 0.1$.

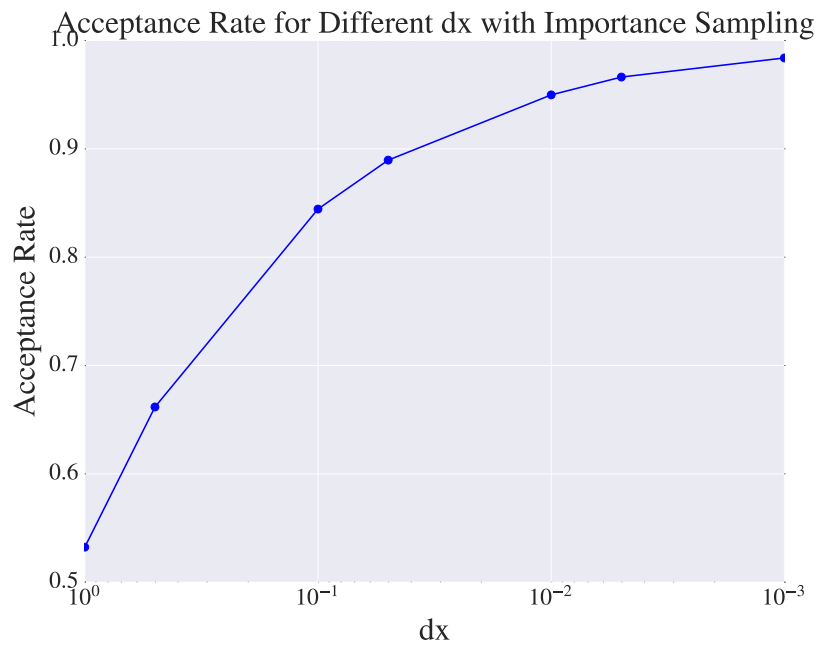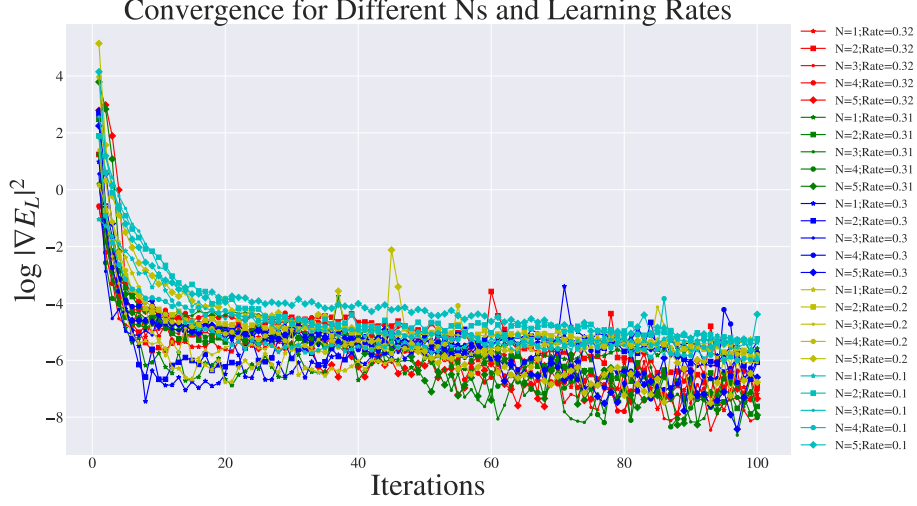(a) The natural logarithm of the square gradient of the local energy.
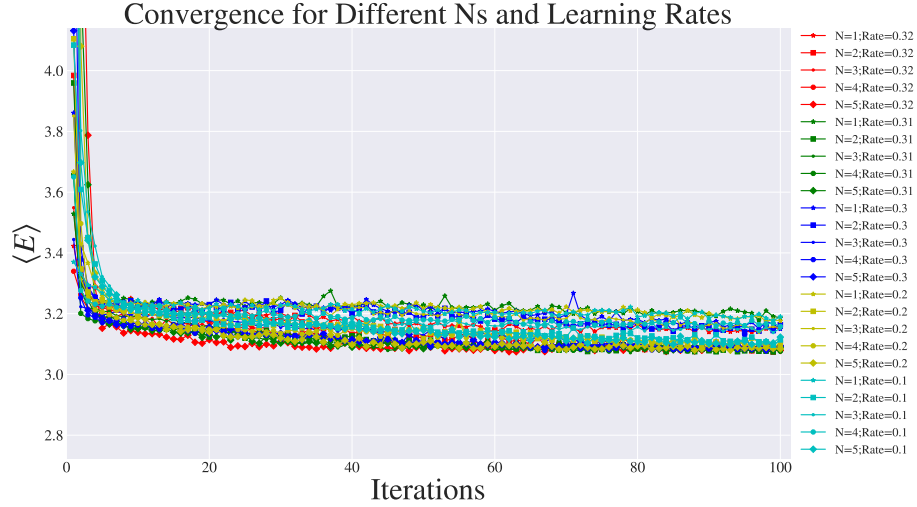
(b) Energy

Figure 8: Plot of the absolute value of the gradient and the energy as a function of iterations for various values of N and γ. This was performed using brute-force Metropolis sampling, using 2 particles in 2 dimensions and $2^{21}/10$ Monte Carlo cycles. We here used $dx = 0.1$. Our convergence tolerance ϵ was 10^{-5}, and we used a maximum of 100 iterations.

The equivalent plot for importance sampling is shown in figure 9. Here, we chose $N = 4$ and $\gamma = 0.3$, as explained in section 5.1.2.

Convergence for Different Ns and Learning Rates with Importance Sampling

(a) The natural logarithm of the square gradient of the local energy.

Convergence for Different Ns and Learning Rates with Importance Sampling

(b) Energy

Figure 9: Same as figure 8, but using importance sampling and therefore $dx = 0.1$.

Finally, the same plot for Gibbs sampling is shown in figure 10. As explained in section 5.1.2, we here choose $N = 2$ and $\gamma = 0.35$.

Convergence for Different Ns and Learning Rates with Gibbs Sampling

(a) The natural logarithm of the square gradient of the local energy.

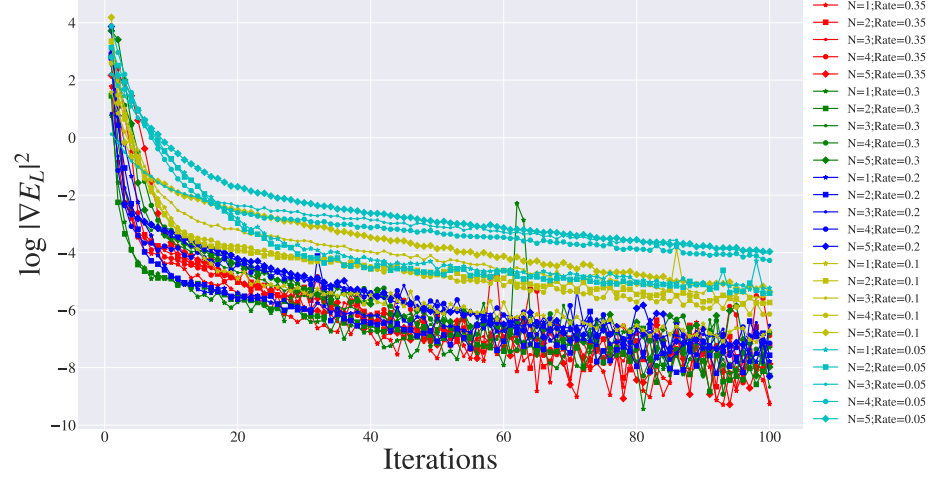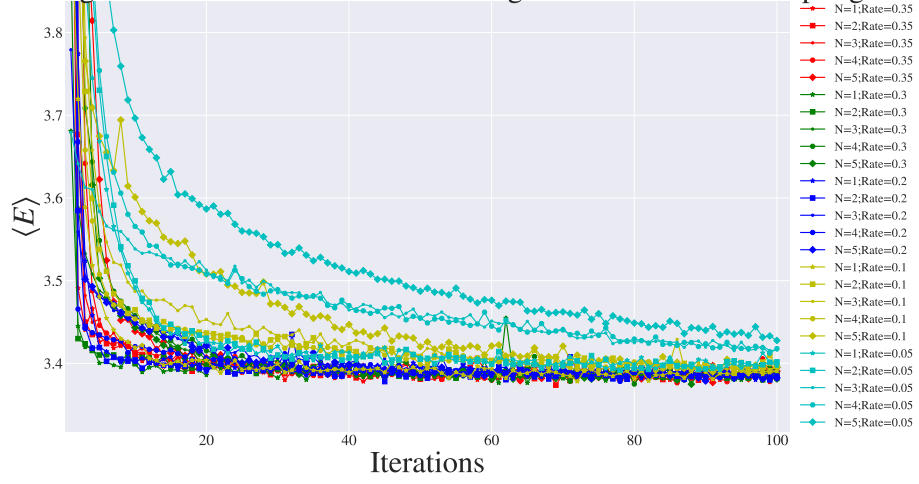Convergence for Different Ns and Learning Rates with Gibbs Sampling

(b) Energy

Figure 10: Same as figure 8 but using Gibbs sampling.

4.3 Results for the tuned system

4.3.1 The noninteracting system

For the noninteracting system, we find the energy for 1, 2 and 3 dimensions. The result is shown in table 1.

Table 1: Results for the noninteracting system with 1 particle, using the tuned parameters described in section 4.1. We use 2^{21} Monte Carlo cycles, and a convergence tolerance ϵ of 10^{-3} with a maximum of 100 iterations. The error is estimated using the blocking method.

Dimension	Type	Mean $[\hbar\omega]$	Error $[\hbar\omega]$	Time[s]
1D	Analytic answer	0.5	-	-
	Brute Force	0.50002	$4.9 \cdot 10^{-9}$	8.27
	Importance	0.500006	$1.9 \cdot 10^{-11}$	11.50
	Gibbs	0.625	$1.3 \cdot 10^{-7}$	10.84
2D	Analytic answer	1.0	-	-
	Brute Force	1.00078	$1.3 \cdot 10^{-8}$	24.72
	Importance	1.0026	$8.7 \cdot 10^{-9}$	49.55
	Gibbs	1.251	$2.7 \cdot 10^{-7}$	26.73
3D	Analytic answer	1.5	-	-
	Brute Force	1.4995	$2.7 \cdot 10^{-8}$	31.02
	Importance	1.505	$1.9 \cdot 10^{-8}$	62.28
	Gibbs	1.875	$4.0 \cdot 10^{-7}$	34.64

4.3.2 The interacting system

The results for the interacting system with two particles is shown in table 2. We only do this in 2 dimensions, as discussed in section 5.3.2.

Table 2: Results for the interacting system in two dimensions, using the parameter tunings from section 4.2. We used 2^{21} Monte Carlo cycles, and a convergence tolerance ϵ of 10^{-3} with a maximum of 100 iterations. The error was estimated using the blocking method.

	Mean $[\hbar\omega]$	Error $[\hbar\omega]$	Time [s]
Analytic answer	3.0	-	-
Brute Force	3.1044	$3 \cdot 10^{-5}$	40.29
Importance	3.090	$4 \cdot 10^{-4}$	118.99
Gibbs	3.887	$4 \cdot 10^{-6}$	58.5

5 Discussion

5.1 Tuning the parameters

5.1.1 The noninteracting case

In the noninteracting case, our chosen parameters are summarized in table 3.

Table 3: Chosen parameters in the noninteracting case

Type	dx	γ	N
Brute-force	0.5	0.3	2
Importance	0.5	0.1	2
Gibbs	-	0.3	2

The step size   We choose the step size in the brute force case by looking at figure 1. We reach the lowest energy for $dx = 0.5$, and it also gives an acceptance rate that is large (which avoids wasting CPU cycles) but not too large (the system does not get stuck). This motivates our choice of dx.

In the interacting case, we determine dx from figure 2. Here, the choice is somewhat more ambiguous. All values of dx give excellent results (they are close to the exact value), though there appears to be an odd behavior for low dx, as it seems to (slightly) violate the variational principle. As the acceptance rate is very high for the lowest dx, however, this effect is unphysical, though it still should not be possible. We therefore choose $dx = 0.5$, as this gives the lowest physical energy.

The learning rate and the number of hidden nodes   For the brute force method, the learning rate and number of hidden nodes are determined from figure 3. We note that the fastest convergence is achieved for 1 hidden node. As this negates the effect of having a NQS however, we choose to consistently neglect the $N = 1$ possibility. The next best convergence with the brute force method was achieved for $\gamma = 0.3$ and $N = 2$, which is what we choose. We also note from figure 3 that all combinations of γ and N eventually end up close to the exact analytic answer. This demonstrates that the choice of learning rate and hidden nodes is not crucial to the success of the system, given that the learning rate is not chosen too low (as can be seen in the cyan curve in figure 3). We also investigated higher learning rates, but found that the system no longer converged consistently.

For importance sampling, we determine the learning rate and the number of hidden nodes from figure 4. For the reasons outlined above, we ignore the run with 1 hidden node, and realize that the fastest convergence is achieved for $\gamma = 0.1$ and 2 hidden nodes, which is what we choose. We once again note that all methods eventually converge close to the exact analytic answer, indicating that this choice is not crucial in this simple system.

Finally, for Gibbs sampling, we choose γ and N from figure 5. Here it is not at all obvious which method gives best convergence. It appears as if $\gamma = 0.4$ and $\gamma = 0.3$ give approximately equally good results. We find, however, that increasing γ only slightly above 0.4 results in the method not converging, and that $\gamma = 0.4$ does not consistently produce good results in higher dimensions. As all choices of parameter (except perhaps a γ of 0.05) appear to converge to the same energy, we choose the rate of 0.3 to ensure convergence in all cases. For $\gamma = 0.3$, it is not clear whether to prefer $N = 2$ or $N = 4$, but as the system only has one degree of freedom, 4 hidden nodes may result in significant overfitting. We therefore choose $N = 2$.

5.1.2 The interacting case

We summarize our chosen parameters in the interacting case (2 particles in 2 dimensions) in table 4.

Table 4: Chosen parameters in the noninteracting case

Type	dx	γ	N
Brute-force	1	0.3	2
Importance	0.1	0.3	4
Gibbs	-	0.35	2

The step size We choose the step size in the brute force case by looking at figure 6. Note that we reach the lowest energy for $dx = 0.1$, but that this has a very high acceptance rate, which may lead to our system getting stuck. We therefore instead choose $dx = 1$, as this has a low energy whilst also having a decent acceptance rate.

In the interacting case, we determine dx from figure 7. Here the choice is clearer: the lowest energy is attained for $dx = 0.1$, and it also has a decent acceptance rate. We therefore choose $dx = 0.1$.

The learning rate and the number of hidden nodes For the brute force method, the learning rate and number of hidden nodes are determined from figure 8 . Here it is not at all clear which N and γ to choose. Choosing γ slightly larger than 0.32 resulted in the method not converging. As there does not appear to be a large difference between $\gamma = 0.32$ and $\gamma = 0.3$, we choose $\gamma = 0.3$, to ensure convergence. It is equally unclear which N to choose, as the absolute value of the gradient fluctuates for al of them. Looking at the energy, shows a cluster of possible, good, values for N which oscillate. We choose $N = 2$, as this is part of this cluster.

For importance sampling, we determine the learning rate and the number of hidden nodes from figure 9. Here, the run with the lowest value for the gradient is $\gamma = 0.3$ and $N = 2$, but this run does not attain a particularly low energy. Instead, we choose the run with $\gamma = 0.3$ and $N = 4$, as this also has a small gradient, but is amongst the runs which attains the lowest energy.

Finally, for Gibbs sampling, we choose γ and N from figure 10. Here, the lowest absolute value of the gradient is attained for $\gamma = 0.35$, though it is not entirely clear which N to choose. We decide to use $N = 2$, to avoid overfitting and because this gives a low value of the gradient and of the energy. Note that we also attempted to use rates higher than $\gamma = 0.35$, but once the rate exceeded 0.4, the method no longer converged.

Note that the gradient generally is much larger in the interacting case than in the noninteracting case, and none of our runs managed to hit the tolerance for the gradient. This is not surprising, as the number of biases and weights is far larger in this case. As such, it may have been sensible to decrease the tolerance in this case.

5.2 Choosing the initial distributions

We note that we have to choose the initial distribution of our particles, our weights/biases and our tuning parameters. We do not present a systematic investigation into the effect of changing these distributions, but note that they do have a significant impact on our result. In particular, we observe that choosing our initial weights/biases to be closer to zero leads to our methods finding the minimum, but then oscillating back and forth quite heavily. We interpret this to be due to the fact that we then do not actually train our NQS. Furthermore, placing our particles closer

together initially leads to a similar result. Note however, that all of these effects are of course not independent of one another, and we have only been able to explore a fairly limited range of our parameter space.

5.3 Results with the tuned parameters

5.3.1 The noninteracting case

The results with the tuned parameters are shown in table 1. We note that the brute force method and importance sampling method both are relatively close to the exact answer, as the relative error in the 1D case is less than 1‰. In the three dimensional case, the largest relative error is about 3% (in the 2D case), but we note that we did not fine-tune our parameters to this case, so it may still be possible to improve this. Note, however, that the blocking error is fair smaller, suggesting that these errors are not due to the lack of statistics. One unsettling point is that the brute force sampling method is able to breach the upper bound set by the variational principle in three dimensions, albeit only slightly. This suggests that there may be a minor bug in our code. This may also have caused the slight violation of the variational principle in figure 2. We have not been able to trace the source of this error.

The Gibbs sampling method gives a significantly larger systematic error, which in each case is about 25%. These results are also consistent with figures 3, 4 and 5, indicating that this effect is not due to our choice of parameters.

The most likely explanation for this effect comes from considering the differences in the wavefunctions used in brute force or importance sampling as opposed to Gibbs sampling. Our trial wavefunction in equation 9 can be made equal to the exact wavefunction for the harmonic oscillator potential by choosing $a_i = b_i = w_{ij} = 0$. As we fix σ to equal 1, however, we cannot achieve this with the wavefunction used in Gibbs sampling ($\sqrt{F_{rbm}}$) as we cannot scale the exponent correctly. This may explain the difference between the methods, and also indicates that Gibbs sampling could benefit from incorporating a variable σ, to enable scaling the exponent of the trial wavefunction.

5.3.2 The interacting case

The results from the interacting case are shown in table 2. These display a similar trend as the results from the interacting case, and many of the same considerations apply. In this case, however, the brute force and importance sampling method produces far worse results (systematic errors on the scale of 3% in the fine-tuned case). Note that we in this case do not know the exact analytic wavefunction, and there is therefore no reason to expect a perfect agreement with the analytic result. We once again note that Gibbs sampling performs much poorer than either brute force or importance sampling, which may indicate that the wavefunction used in Gibbs sampling is a poorer approximation of the exact wavefunction of the system.

We attempted to run this system also for 1 and 3 dimension, but our method did not converge consistently. This suggests that the interacting case is much more sensitive to the parameters that we tune than the noninteracting case, and one would have to perform a separate tuning of these parameters in this case. It also suggests that it is difficult to generalize the NQS, at least in the form presented here, to more particles or dimensions as it is so sensitive to the chosen tuning parameter values.

6 Conclusion

6.1 Conclusion

We have investigated the use of Neural-network Quantum States (NQS) in modelling quantum mechanical systems. We look at fermions in an isotropic harmonic oscillator potential, and present and compare three different sampling methods to use with our NQS: brute-force Metropolis sampling, importance sampling (Metropolis-Hastings algorithm) and Gibbs sampling. In each of these cases, we tweaked the parameters of our system to achieve a good rate of convergence and a low energy.

We have found that brute-force sampling and importance sampling perform about equally well with NQS, but Gibbs sampling performs much poorer. However, we also find that our system is very sensitive to the initial distribution and fine-tuning of our parameters. As the above conclusions are only based on investigation of a fairly restricted part of parameter space, they may not be universally valid.

We looked at a system of a single fermion in 1, 2 and 3 dimensions, and a system of two fermions in 2 dimensions. In the single fermion case the results are shown in table 1. For brute force and importance sampling, the error is in all cases less than 3%, whereas the error with Gibbs sampling is about 25%. In the two fermion case, shown in table 4, the errors are somewhat larger in both cases, though Gibbs still performs poorly compared to brute-force and importance sampling. In all cases, the statistical error is too small to explain the discrepancy, so there is a systematic error. More worryingly, however, is that we manage to (slightly) violate the variational principle in the 3D case with 1 fermion. This suggests that there may be a small unnoticed bug in our code.

6.2 Outlook

There is still significant work needed to determine the ultimate usefulness of Neural-network Quantum States.

One particular interesting investigation would be varying the σ (spread in the visible nodes) in the wavefunction as, if our reasoning in section 5.3.2 is correct, this may lead to significantly better results for Gibbs sampling.

It may also be very interesting to automate our method further, employing a minimization method not just to the weights, but also to dx, γ, N and even σ. Note, however, that this may require a more sophisticated optimization method. This may make it possible to avoid the tedious manual tuning of parameter, and may give us better results in the higher-dimensional case. In addition, however, the system is also highly sensitive to the initial distribution of the parameters, and thus some manual tuning will most likely be required anyhow.

Finally, it would be of great interest to investigate why our method appears to sometimes slightly violate the variational principle. If this bug is found, then we may attain some improvement of our results.

References

[Botu and Ramprasad, 2015] Botu, V. and Ramprasad, R. (2015). Adaptive machine learning framework to accelerate ab initio molecular dynamics. *International Journal of Quantum Chemistry*, 115(16):1074–1083.

[Broecker et al., 2017] Broecker, P., Carrasquilla, J., Melko, R. G., and Trebst, S. (2017). Machine learning quantum phases of matter beyond the fermion sign problem. *Scientific Reports*, 7(1):8823.

[Carleo and Troyer, 2017] Carleo, G. and Troyer, M. (2017). Solving the quantum many-body problem with artificial neural networks. *Science*, 355(6325):602–606.

[Griffiths, 2004] Griffiths, D. (2004). *Introduction to Quantum Mechanics*. 2 edition.

[Heinesen et al., 2018] Heinesen, D., Lange, G., and Salihi, A. (2018). FYS4411 - Project 1 Variational Monte Carlo.

[Hinton, 2010] Hinton, G. (2010). A Practical Guide to Training Restricted Boltzmann Machines. Technical report, University of Toronto, Toronto.

[Hjorth-Jensen, 2015] Hjorth-Jensen, M. (2015). *Computational Physics*. Oslo.

[Hjorth-Jensen, 2018] Hjorth-Jensen, M. (2018). Project 2, The restricted Boltzmannn machine applied to the quantum many body problem.

[Jonsson, 2018] Jonsson, M. (2018). *LECTURE NOTES FOR BLOCKING METHOD*.

[Pedersen Lohne et al., 2011] Pedersen Lohne, M., Hagen, G., Hjorth-Jensen, M., Kvaal, S., and Pederiva, F. (2011). Ab initio computation of the energies of circular quantum dots. *Phys. Rev. B*, 84(11):115302.

[Taut, 1994] Taut, M. (1994). Two electrons in a homogeneous magnetic field: particular analytical solutions. *Journal of Physics A: Mathematical and General*, 27(3):1045.

[Wang et al., 2014] Wang, N., Melchior, J., and Wiskott, L. (2014). Gaussian-binary Restricted Boltzmann Machines on Modeling Natural Image Statistics.

Appendices

A Finding the derivatives

In this section, we derive the expressions for the various derivatives needed in section 2. We begin with the local energy.

A.1 The local energy

The local energy is given by:

$$E_L = \frac{1}{\Psi_T}\hat{H}\Psi_T = \sum_{i=1}^{N}\left(-\frac{1}{2\Psi_T}\nabla_i^2\Psi_T + \frac{1}{2}\omega^2 r_i^2\right) + \sum_{i<j}\frac{1}{r_{ij}} \tag{29}$$

Thus, we must compute:

$$\frac{1}{\Psi_T}\nabla_i^2\Psi_T \tag{30}$$

This may be rewritten as:

$$\frac{1}{\Psi_T}\nabla\left(\Psi_T\frac{1}{\Psi_T}\nabla\Psi_T\right) = \left(\frac{1}{\Psi_T}\nabla\Psi_T\right)^2 + \nabla\left(\frac{1}{\Psi_T}\nabla\Psi_T\right) = \left[\nabla\log\Psi_T\right]^2 + \nabla^2\log\Psi_T \tag{31}$$

The logarithm of our trial wavefunction is given by:

$$\log\Psi_T = -\log Z - \sum_{i=1}^{M}\left(\frac{(X_i - a_i)^2}{2\sigma^2}\right) + \sum_{j=1}^{N}\log\left(1 + \exp\left(b_j + \sum_{i=1}^{M}\frac{X_i w_{ij}}{\sigma^2}\right)\right) \tag{32}$$

The derivative with respect to one coordinate is now given by:

$$\begin{aligned}
\frac{\partial\log\Psi_T}{\partial X_k} &= \frac{(a_k - X_k)}{\sigma^2} + \sum_{j=1}^{N}\frac{w_{kj}\exp\left(b_j + \sum_{i=1}^{M}\frac{X_i w_{ij}}{\sigma^2}\right)}{\sigma^2\left(1 + \exp\left(b_j + \sum_{i=1}^{M}\frac{X_i w_{ij}}{\sigma^2}\right)\right)} \\
&= \frac{a_k - X_k}{\sigma^2} + \sum_{j=1}^{N}\frac{w_{kj}}{\sigma^2\left(1 + \exp\left(-b_j - \sum_{i=1}^{M}\frac{X_i w_{ij}}{\sigma^2}\right)\right)}
\end{aligned} \tag{33}$$

Whereas the second derivative is:

$$\frac{\partial^2\log\Psi_T}{\partial X_k^2} = -\frac{1}{\sigma^2} + \sum_{j=1}^{N}\frac{w_{kj}^2\exp\left(-b_j - \sum_{i=1}^{M}\frac{X_i w_{ij}}{\sigma^2}\right)}{\sigma^4\left(1 + \exp\left(-b_j - \sum_{i=1}^{M}\frac{X_i w_{ij}}{\sigma^2}\right)\right)^2} \tag{34}$$

The local energy can now be found by using equation 31, and inserting equation 33 and equation 34. Inserting this into equation 29 gives the expression for the local energy stated in the main text.

A.2 The derivatives with respect to the parameters

For our optimization method, we require:

$$\frac{1}{\Psi_T}\frac{\partial\Psi_T}{\partial\alpha_k} = \frac{\partial}{\partial\alpha_k}\log\Psi_T \tag{35}$$

Where α_k is any of the biases a, b or the weights w of the restricted Boltzmann machine. These derivatives are given by:

$$\frac{\partial \log \Psi_T}{\partial a_k} = \frac{X_k - a_k}{\sigma^2} \tag{36}$$

$$\frac{\partial \log \Psi_T}{\partial b_k} = \frac{\exp\left(b_k + \sum_{i=1}^{M} \frac{X_i w_{ik}}{\sigma^2}\right)}{1 + \exp\left(b_k + \sum_{i=1}^{M} \frac{X_i w_{ik}}{\sigma^2}\right)} = \frac{1}{1 + \exp\left(-b_k - \sum_{i=1}^{M} \frac{X_i w_{ik}}{\sigma^2}\right)} \tag{37}$$

Finally, the derivative with respect to the coupling weights, w_{kl} is given by:

$$\frac{\partial \log \Psi_T}{\partial w_{kl}} = \frac{X_k \exp\left(b_l + \sum_{i=1}^{M} \frac{X_i w_{il}}{\sigma^2}\right)}{\sigma^2 \left(1 + \exp\left(b_l + \sum_{i=1}^{M} \frac{X_i w_{il}}{\sigma^2}\right)\right)} = \frac{X_k}{\sigma^2 \left(1 + \exp\left(-b_l - \sum_{i=1}^{M} \frac{X_i w_{il}}{\sigma^2}\right)\right)} \tag{38}$$

A.3 The derivatives with Gibbs sampling

In Gibbs sampling, we represent the wavefunction as $\Psi_{T,\text{Gibbs}} = \sqrt{F_{rbm}(\boldsymbol{X})}$, instead of $\Psi_T = F_{rbm}(\boldsymbol{X})$. Note, however, that we only ever differentiate the logarithm of the wavefunction. As $\log \sqrt{\Psi_T} = \frac{1}{2} \log \Psi_T$, this gives only a marginal change. Specifically:

$$E_L = [\nabla \log \sqrt{\Psi_T}]^2 + \nabla^2 \log \sqrt{\Psi_T} = \frac{1}{4}[\nabla \log \Psi_T]^2 + \frac{1}{2}\nabla^2 \log \Psi_T \tag{39}$$

$$\frac{\partial}{\partial a_k} \log \sqrt{\Psi_T} = \frac{1}{2}\frac{\partial}{\partial a_k} \log \Psi_T \tag{40}$$

$$\frac{\partial}{\partial b_k} \log \sqrt{\Psi_T} = \frac{1}{2}\frac{\partial}{\partial b_k} \log \Psi_T \tag{41}$$

$$\frac{\partial}{\partial w_{kl}} \log \sqrt{\Psi_T} = \frac{1}{2}\frac{\partial}{\partial w_{kl}} \log \Psi_T \tag{42}$$

Where the derivatives on the right-hand side are given in the previous section.

B Deriving the spin of the ground state wavefunction

In this section we derive the spin of the exact two-particle ground state wavefunction in the non-interacting case.

Consider the unperturbed wavefunction for the ground state of the two electron system, given by:

$$\psi(\boldsymbol{r}_1, \boldsymbol{r}_2) = C \exp\left(-\omega \left(r_1^2 + r_2^2\right)/2\right) \tag{43}$$

Since this wavefunction is symmetric under permutation of coordinate, the Pauli exclusion principle states that the spin wavefunction must be antisymmetric function in to achieve a wavefunction that is totally antisymmetric under permutation of coordinates. This wave function must then be the singlet, and will look like:

$$|\psi\rangle = \frac{1}{\sqrt{2}}\left(|\uparrow\rangle - |\downarrow\rangle\right) \tag{44}$$

This has spin 0, as can be seen by applying the spin operator $\boldsymbol{S}^2$ to this state:

$$\boldsymbol{S}^2|\psi\rangle = \frac{1}{\sqrt{2}}\left(\underbrace{\boldsymbol{S}^2|\uparrow\rangle}_{=\frac{3}{4}\hbar^2} - \underbrace{\boldsymbol{S}^2|\downarrow\rangle}_{=\frac{3}{4}\hbar^2}\right) = 0 \tag{45}$$